Chem Soc Rev

This article was published as part of the

2008 Chemistry at Surfaces issue

Reviewing the latest developments in surface science

All authors contributed to this issue in honour of the 2007 Nobel Prize winner Professor Gerhard Ertl

Please take a look at the issue 10 table of contents to access the other reviews

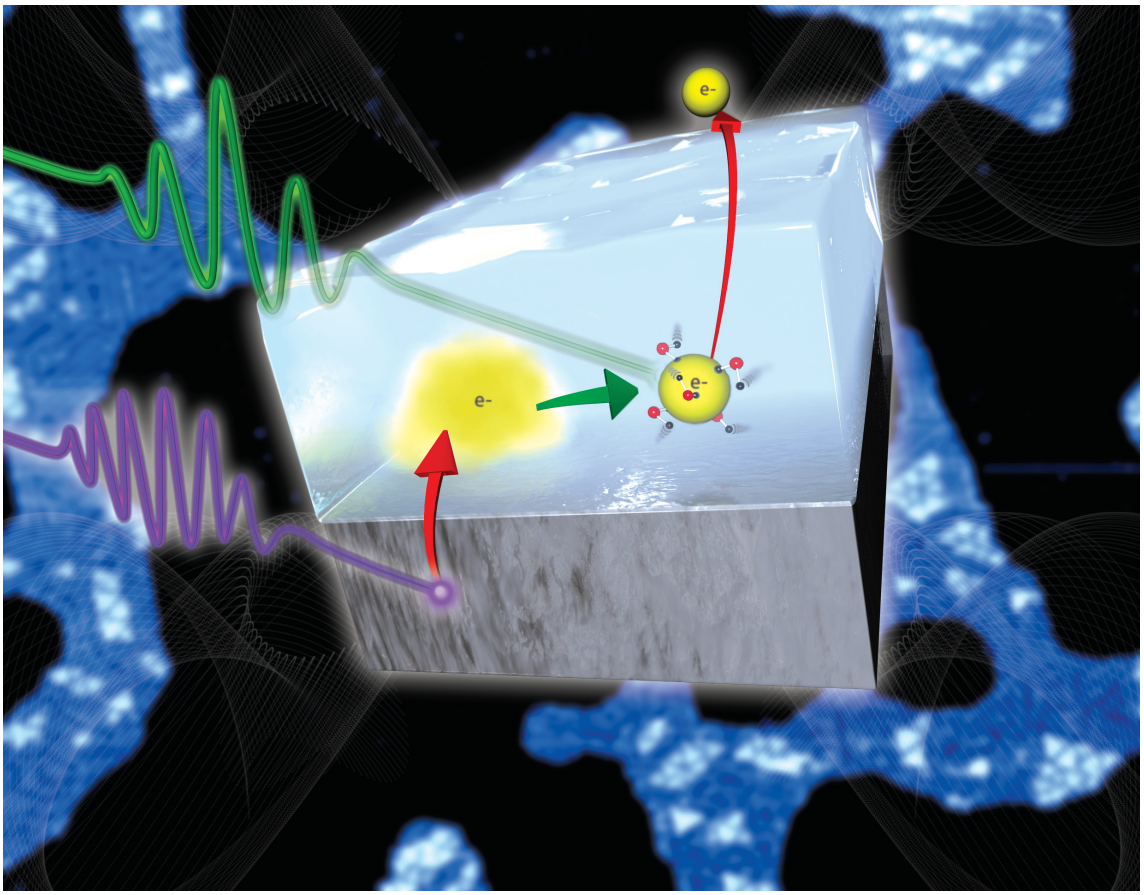

The nature of the active site in heterogeneous metal catalysis†

Jens K. Nørskov,*[a] Thomas Bligaard,[a] Britt Hvolbæk,[a] Frank Abild-Pedersen,[ab] Ib Chorkendorff[c] and Claus H. Christensen[d]

Received 9th May 2008
First published as an Advance Article on the web 4th August 2008
DOI: 10.1039/b800260f

This *tutorial review*, of relevance for the surface science and heterogeneous catalysis communities, provides a molecular-level discussion of the nature of the active sites in metal catalysis. Fundamental concepts such as "Brønsted–Evans–Polanyi relations" and "volcano curves" are introduced, and are used to establish a strict partitioning between the so-called "electronic" and "geometrical" effects. This partitioning is subsequently employed as the basis for defining the concept "degree of structure sensitivity" which can be used when analyzing the structure sensitivity of catalytic reactions.

Introduction

Metal surfaces are used extensively as catalysts in all sections of chemical industry, in environmental protection and in energy conversion processes. Typically, the metals are present in the form of nanoparticles in order to expose as large a surface area as possible to the reacting molecules from the gas or liquid phase. Nanoparticles larger than a few nanometres are often found in "*in situ*" experiments[1–4] to be nicely crystalline exposing well-defined surfaces together with a number of other configurations of metal atoms—steps, kinks, edges, and corners. An important question is which of these local geometries constitute the active sites where the catalysis actually takes place. Related to this is the question of the origin of the structure dependence of reaction rates as observed for instance through the variations of the catalytic activity with particle size.

The question of the nature of the active sites and structure dependence of heterogeneous catalysts has been debated for almost a century,[5–17] dating back to the suggestion by Taylor that unsaturated active sites at the atomic level can control the surface chemical reactivity.[5] Boudart went on to classify reactions in terms of their structure sensitivity or structure insensitivity.[6,7] The understanding of the structure dependence of reactions has progressed enormously with the development of ultra-high vacuum technology combined with single crystal studies.[9] Somorjai,[10,11] Yates,[12,13] and their co-workers have used such surface science studies to demonstrate and analyze in detail the enhanced chemical activity of step sites compared to close-packed surfaces. This has led to the first direct STM observations of the active sites for the NO dissociation reaction over atomically resolved stepped ruthenium surfaces by Ertl and co-workers.[14] Recently, gold nano-effects[18] has become one

[a] *Center for Atomic-scale Materials Design (CAMD), Department of Physics, Building 307, Technical University of Denmark, DK-2800 Kgs. Lyngby, Denmark. E-mail: norskov@fysik.dtu.dk*
[b] *Computational Materials Design ApS, Matematiktorvet 307, DK-2800 Kgs. Lyngby, Denmark*
[c] *Center for Individual Nanoparticle Functionality (CINF), Department of Physics, Building 312, Technical University of Denmark, DK-2800 Kgs. Lyngby, Denmark*
[d] *Center for Sustainable and Green Chemistry (CSG), Department of Chemistry, Building 206, Technical University of Denmark, DK-2800 Kgs. Lyngby, Denmark*
† Part of a thematic issue covering reactions at surfaces in honour of the 2007 Nobel Prize winner Professor Gerhard Ertl.

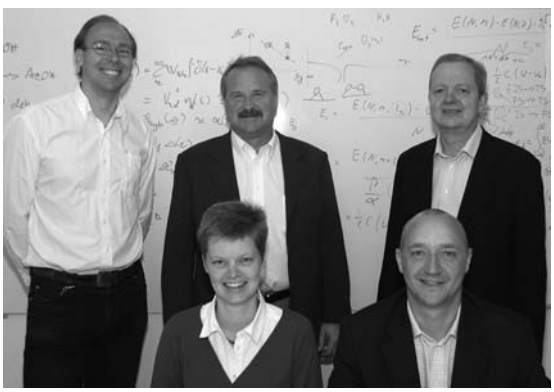

Back row from the left: Thomas Bligaard, Ib Chorkendorff and Jens K. Nørskov. Front row: Britt Hvolbæk and Claus H. Christensen

The research in surface science and heterogeneous catalysis at the Technical University of Denmark (DTU) is organized in three research centers with strong interrelations. Professor Jens K. Nørskov is the director of the Center for Atomic-scale Materials Design (CAMD) and is also the director of NanoDTU which is the interdisciplinary nanotechnology center at DTU. Professor Ib Chorkendorff is the director of the Center for Individual Nanoparticle Functionality (CINF). Professor Claus H. Christensen is the director of the Center for Sustainable and Green Chemistry (CSG). Dr Britt Hvolbæk is the vice director of NanoDTU. Dr Frank Abild-Pedersen is the Chief Technology Officer in the start-up company Computational Materials Design ApS. Assistant professor Thomas Bligaard is the group leader of theoretical surface science and materials informatics at CAMD.

of the hottest areas in catalysis research, and the origin of the activity and the nature of the active sites is a topic currently under intense debate.[19–21] It was only after theoretical methods based on density functional theory calculations were developed into a semi-quantitative tool in describing surface reactivity,[22] and the calculations were coupled to careful experiments, that it became clear that there could be many orders of magnitude differences in reaction rates for different surface structures.[15]

In the present review, we provide a molecular level discussion of the nature of the active sites in metal catalysis. We will show how different classes of reactions have different active sites and different dependence of the catalytic activity (turn over rate and/or selectivity) on particle size. We will start by introducing the key concepts in our analysis: the Brønsted–Evans–Polanyi (BEP) relationship between activation energies and reaction energies for elementary surface reactions. They determine the trends in catalytic activity from one metal to the next—the so-called volcano relationships. The dependence of the BEP lines on the local structure of the reaction site determines the structure sensitivity (or geometrical effect) of the individual elementary reactions and it also determines whether a complete catalytic reaction will exhibit structure sensitivity for a given catalyst. We define on this basis a term that we call the "degree of structure sensitivity", which can be used to quantify the effect.

BEP relations in surface reactions

The discussion in the following is based on the assumption that supported metallic nanoparticles in a high surface area catalyst can be viewed as consisting of a distribution of surfaces with different local geometries—different facets or edges, corners, steps and kinks. This is a good approximation for metals where screening by the itinerant electrons introduces a so-called "nearsightedness"[23,24] such that a perturbation to the surface is only measurable within a screening length—typically a few ångstroms or on the order of one lattice constant. For very small particles, where the electrons are no longer itinerant this picture breaks down—the exact size where this happens is still an open question. The nearsightedness means that different types of surface sites or local geometries can be viewed as independent of each other. It also means that the effect of the support is restricted to the region very close to the interface between the metal particle and the support. Such effects can be interesting, but we will not discuss them further here. The support effects that we are implicitly including in the present treatment are thus those related to the way the support influences the size and shape of the catalytic metallic nanoparticles.

Any catalytic reaction consists of a series of elementary reactions. We will study the effect of different local geometries on the rate of different types of elementary surface reactions one by one, and then put this together in a description of structural effects for complete reactions.

There are two ways in which the geometrical structure can affect the stability of reaction intermediates and the activation energy of a chemical reaction. One effect is entirely electronic and the other effect is purely geometrical.

The electronic effect is due to the surface metal atoms in different environments having slightly different local electronic structures and they hence interact differently with molecules both when these adsorb and when they react. For transition metals, it has been found quite generally that the d-band center—the first moment of the density of states projected onto the d-orbitals for the surface atoms interacting with the adsorbates—is a good measure of the ability of the atoms in question to form bonds to an adsorbate.[25–28] Late transition metal atoms with a low coordination number (open surfaces, steps, edges, kinks and corners) tend to have higher lying d-states and therefore interact more strongly with adsorbates than atoms on close packed surfaces with a high metal coordination number.

The purely geometrical effect comes from different surface geometries providing different configurations to the molecule for bonding.[29] It is in general difficult to differentiate the two effects: steps, for instance offer atoms with higher-lying d-states than close packed surfaces and at the same time they offer new surface atom configurations. One way to separate the two effects is by plotting the activation energy for a surface chemical reaction as a function of the reaction energy for a range of metals and for different surface geometries, as illustrated in Fig. 1.

Activation energies for surface reactions are often found to be roughly linear functions of the reaction energy:[29,30]

$$E_a = \alpha\Delta E + \beta \qquad (1)$$

Fig. 1 shows examples of such plots—Brønsted–Evans–Polanyi lines or BEP lines—for two dissociative adsorption reactions. Such linear scaling between transition states and adsorption energies can be viewed as resulting from both the transition state and the adsorbates having adsorption energies that are linearly dependent on the d-band center.[28] For some reactions such as the dissociation of methane, Fig. 1a, essentially the same linear relation is found for different surface geometries. There can still be electronic step effects—observe for instance how the Ni(211) point is shifted to the left of the Ni(111) point. This is an example of the d-band effect discussed above: the step atoms on the (211) surface (see inset) have a lower metal coordination number and hence higher lying d-states than the Ni atoms on the close packed (111) surface. This leads to stronger bonding of the intermediates as well as the transition state. The electronic effect thus corresponds to a displacement along the BEP line.

For other reactions, there are large shifts in the BEP lines for different geometries. This is shown for N_2 dissociation in Fig. 1b. Such strong effects are found generally for N–O, C–O, O–O, N–N,[29] and C–C bond scission.[17] It is found that open surfaces and in particular some kinds of steps have particularly low-lying BEP lines (low β values, *cf.* eqn(1)).

Similar BEP lines have been found for reactions between surface species and for desorption reactions. The latter are simply the reverse of the adsorption reactions like those included in Fig. 1, and since $E_{a,desorption} = E_{a,adsorption} - \Delta E$, we have from eqn (1) that $\alpha_{desorption} = \alpha_{adsorption} - 1$.

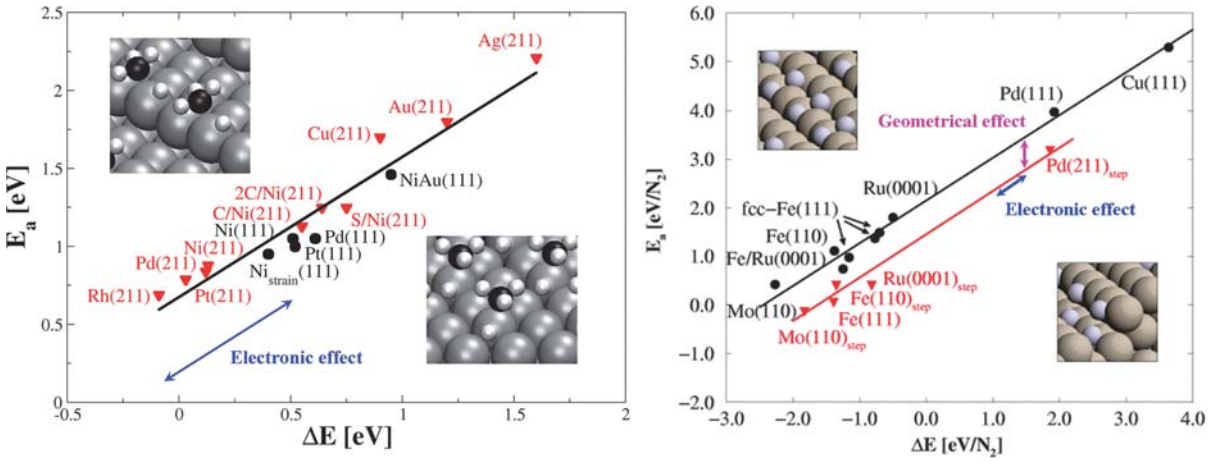

Fig. 1 (a) The BEP relationships for dehydrogenation of methane over a number of fcc (211) and (111) transition metal surfaces. The stepped surfaces show a slightly higher dissociation barrier than the (111) surfaces at a given reaction energy (dissociative chemisorption energy), but the electronic effect is much larger than the geometrical effect, $\delta\beta \ll \delta\Delta E$. (b) The BEP relationships for N_2 dissociation over a number of stepped and close-packed surfaces. The BEP line for open surfaces lies significantly below that of the close-packed surfaces (on the order of 1 eV). At a given reactivity of the surface, N_2 thus prefers splitting over the under-coordinated sites at the steps.[15] Here the geometric effect is larger than the electronic effect, $\delta\beta \gg \delta\Delta E$.

Strongly adsorbed atoms like N, C or O usually prefer the sites with the highest metal coordination number, that is, the same local adsorption geometry on *e.g.* a close packed and a stepped surface. This means that if the point of a given metal shifts on the *x*-axis of Fig. 1 when the geometry changes, this is primarily an electronic effect. It also means that, if we keep the value of the reaction energy fixed, the shift from one BEP line to the next is the purely geometrical effect. In this way, the two effects can be systematically separated.

The size of the geometrical effect depends on the nature of the transition state. The transition state for *e.g.* N_2 dissociation is quite extended, see inset in Fig. 1b, and several metal surface atoms can be used to stabilize it. The step shown in Fig. 1b can use five atoms such that no metal atom needs to bond to more than one of the N atoms during the dissociation. The close-packed surface, on the other hand, can only use four surface atoms and one of the surface atoms needs to help stabilizing both N atoms. This is the reason the step BEP line is below the BEP line for the close-packed surface. We note that the Fe(111) surface, which is extremely open and exposes sites that are very much like the steps on the close-packed Fe(110) surface, is also on the step line.

The fact that there is only a weak geometry-dependence for the reaction in Fig. 1a is also a consequence of the nature of the transition state. When C–H bonds are broken (or formed), the transition state is much less extended than for N–N bond breaking, and the transition state is situated above a single metal atom. This makes the intrinsic geometrical effect small. The size of the geometrical effect is therefore dependent on the nature of the transition state, and for extended transition states different surface structures will give different BEP lines. Often close-packed surfaces give the highest and very open structures like steps the lowest values of β, but this need not be so for all molecules.

We conclude that we can identify three classes of structural dependence for surface reactivity:

Strong structural effects are found when the shift in BEP lines (or shift in β, $\delta\beta$) is large and larger than the shift in reaction energy, $\delta\Delta E$, from one structure to the next. This is a truly geometrical effect and N_2 dissociation is an example of this type of behavior. Other examples include N–O, C–O, O–O, and C–C bond breaking.

Weak structural effects are found when the β-shift is small and the only effect of a change in active site structure is the electronic effect due to a change in reaction energy from one surface structure to the next. Methane activation is an example of this type of behavior and other types of C–H or O–H bond breaking (or making) reactions also belong here.

No structural effects are found when there is no geometry dependence of β and there is no electronic effect. There are not likely to be many such examples, if any.

Exploiting the nearsightedness discussed above, the rate of an elementary reaction on a surface with several different types of sites can be written as:

$$r = \sum_i r_i = \sum_i A_i v_i e^{-E_{ai}/kT} = \sum_i v_i e^{-(E_{ai} - kT \ln A_i)/kT} \quad (2)$$

where A_i is the relative abundance of surface geometry i in the system, v_i is the Arrhenius prefactor, and E_{ai} is the activation energy for this geometry. T is the absolute temperature and k is the Boltzmann constant. Assuming that the prefactors are independent of the geometry, as they have been shown to be in some cases,[31] it is clear that an active site for an elementary reaction can be defined if one site (or class of sites) has an activation energy that is smaller than all others on a scale of kT and taking into account the relative abundance of this particular configuration.

The relative importance of two sites k and l is given by

$$\frac{r_k}{r_l} = \frac{A_k e^{-E_{ak}/kT}}{A_l e^{-E_{al}/kT}} = e^{-\{(E_{ak} - E_{al}) - kT(\ln A_k - \ln A_l)\}/kT} \quad (3)$$

This shows that in order to compare the relative importance of different sites we should compare the geometry probability-weighted activation energies:

$$E_{ai}^{w} = E_{ai} - kT \ln A_i \quad (4)$$

If one of these is smaller than the rest (on the scale of kT) this site will dominate the reaction and the corresponding structure will appear to be the active site. In the following, we will consider examples of elementary reactions where it is possible to identify a well-defined active site.

For a complete catalytic reaction consisting of several elementary reaction steps, it takes a more elaborate analysis to define that active site and to determine the structure dependence of the catalytic rate. To this end, we will first in the following section briefly discuss the relationship between BEP relations and trends in catalytic reaction rates.

From BEP relations to reactivity trends: the Sabatier analysis

It was realized already a century ago that the rate for a heterogeneous catalytic reaction under given conditions shows a maximum when considered as a function of the reactivity of the catalytic surface.[32] In other words, the most active catalyst is neither a very reactive nor a very noble surface, but rather a compromise between these extremes. Modern electronic structure theory allows us to quantify what is meant by "reactivity of the catalytic surface", and thus to analyze the origins of the experimental observations. Here, we discuss how the linear BEP relationships described above can lead directly to volcano curves when the rate is plotted against the reactivity of the catalytic surface as described *e.g.* by the dissociative chemisorption energy of the key reactant.

We consider a simple "generalized" surface-catalyzed reaction not with the aim of describing a particular reaction in detail, but rather to highlight the common features determining catalytic activity for heterogeneous catalysts in general. A heterogeneous catalytic reaction can be viewed in general terms as a number of coupled reaction steps which include adsorption of the reactants, subsequent surface-mediated activation of the reactants followed by surface-mediated recombination and finally removal of the products from the surface. For the simplest reactions, the recombination and removal occurs in a single step.

Fig. 2 shows a sketch of a potential energy diagram for such a simple reaction, corresponding to the reaction equations:

$$A_2 + * \leftrightarrows A_2* \quad (r1a)$$

$$A_2* + * \leftrightarrows 2A* \quad (r1b)$$

$$A* + B \leftrightarrows AB + * \quad (r2)$$

Here the "*" represents a surface site, and *e.g.* A_2* signifies that A_2 is bound to a surface site. If the non-dissociated state of the reactants (the precursor state) is only weakly adsorbed, the adsorption (r1a) and the activation (r1b) of the reactant can be viewed as a single dissociative chemisorption step with an effective activation barrier of E_{a1} relative to the gas phase reactant:

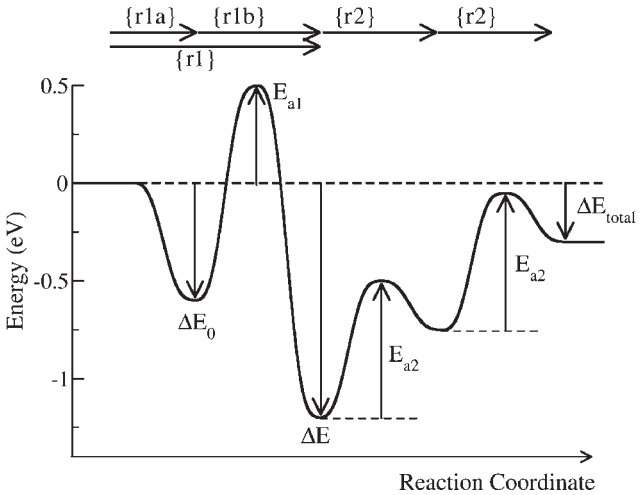

Fig. 2 Schematic potential energy diagram for a surface reaction involving adsorption of A_2, dissociation of A_2, and the removal of A from the surface by two consecutive reactions with B to form two AB molecules from one A_2 and two B "molecules".

$$A_2 + 2* \leftrightarrows 2A* \quad (r1)$$

Reaction (r2) is written as if the gas phase molecule B reacts directly with an adsorbed atom A with an activation barrier of E_{a2}. This should rather be thought of as a generalized reaction, which may involve several elementary steps, including adsorption of B in a different site than A, such that A and B do not compete for coverage.

From the discussion in the previous section, it is clear that there often exists a linear relation between the barrier for dissociative chemisorption, E_{a1}, and the dissociative chemisorption energy, ΔE, and that an equivalent relation often exists for the removal step. The reaction kinetics will thus depend on two coupled linear relations:

$$E_{a1} = \alpha_1 \cdot \Delta E + \beta_1 \quad (5)$$

$$E_{a2} = \alpha_2 \cdot \Delta E + \beta_2 \quad (6)$$

where in most cases α_1 is positive and α_2 is negative. This means that, as the surface becomes more reactive (more negative ΔE), the barrier for activation of the reactants becomes smaller and the barrier for desorption of products becomes larger. Conversely, as the catalytic surface is chosen among the more noble metals (less negative ΔE), the barrier for activation of the reactants becomes large but the removal of products becomes more facile.

It is perhaps not immediately clear that this behavior leads to a volcano relation for the over-all reaction rate, since the different rates are coupled through the coverages of activated reactants and the coverage of free sites. However, exact upper bounds to the reactivity can be established under practical assumptions, and these upper bounds will illustrate the volcano behavior. We refer to such type of analysis as the "Sabatier analysis".[33] Clearly, the over-all reaction rate cannot be larger than the maximal forward rate of the activation step (r1), nor can it be larger than the maximal rate of the removal step (r2). In standard microkinetic modeling,[7] the maximal forward rate for a given step is equal to the rate constant, except from

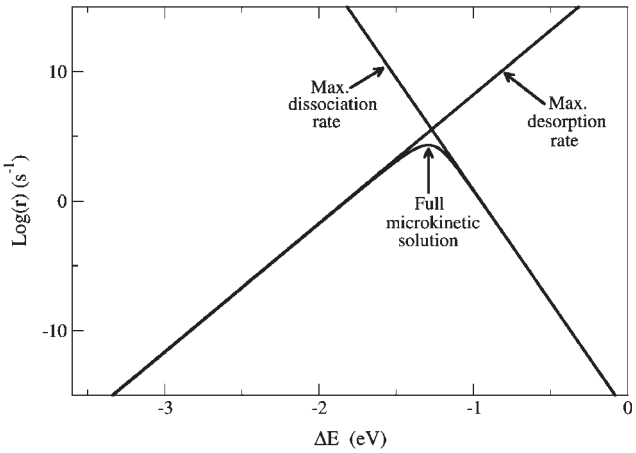

Fig. 3 The Sabatier volcano curve and the full solution to the microkinetic model for the simple generalized heterogeneous catalytic reaction. The parameters $\alpha_1 = 0.89$, $\beta_2 = 1.34$ eV, $\alpha_2 = -0.5$, and $\beta_2 = 0.8$ eV were used. It has been assumed that the reaction enthalpy of the total gas phase reaction is $\Delta E_0 = -1$ eV, but that does not affect the Sabatier curves, only the so-called approach to equilibrium. The full microkinetic solution is shown for reaction conditions far from equilibrium.[33]

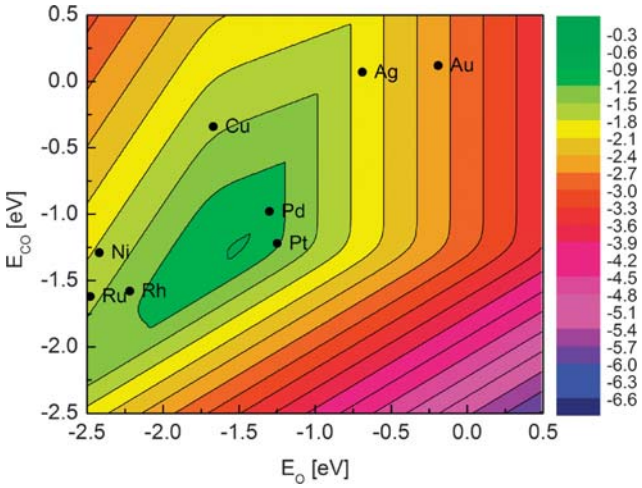

Fig. 4 Contour plot of the Sabatier activity ($kT\cdot\ln(r_s/\upsilon)$) in eV as a function of E_{CO} and E_O (υ is here set equal to kT/h) at close-packed surfaces under high temperature conditions ($T = 600$ K, $P_{O2} = 0.33$ bar and $P_{CO} = 0.67$ bar). The values for different fcc(111) surfaces of elemental metals are indicated as black points. Adapted from ref. 34.

trivial prefactors depending only on coverages and pressures. Coverages maximizing the rate are assumed. This is an exact upper bound, and is often reasonable, since a step being slow will in many cases have a tendency to make the coverage of the involved reactants high. The pressures are of course known from the applied reaction conditions. Due to the linear relations discussed above, the rate constants for the two key reaction steps behave oppositely. This is illustrated in Fig. 3. The maximal rates are shown for the two reaction steps, with a choice of reasonable standard reaction parameters.[33] The exponential variations in the maximal rates of the individual steps are due to the linear variations in the activation barriers in the Arrhenius expressions for the rate constants as ΔE is varied. The maximal rate curves trace out what we call the ''Sabatier volcano''—an exact upper bound on the reaction rate.

The full self-consistent solution to the microkinetic model in the steady state approximation is also shown in Fig. 3. It is seen that under the given choice of reaction conditions (relatively far from equilibrium between reactants and products in the gas phase) the top of the Sabatier volcano coincides exactly with the top of the full solution to the microkinetic model. This is a general observation that the simple Sabatier volcano describes the kinetics well, as long as the reaction is far from equilibrium and the surfaces of optimal reactivity are not poisoned by reactants or products. For reactions which are not equilibrium-limited, the Sabatier analysis is thus often a useful tool for understanding the reactivity of the optimal catalyst. When there are more than two important reaction steps, there can be more than one key descriptor. This occurs when the reactions between the surface intermediates depend on the adsorption of different species whose adsorption energies are not highly correlated. One such example is the CO oxidation reaction where both the adsorption energy of CO molecules and of O atoms becomes important. The adsorption energies of these two atoms do not correlate very well with each other. This means that an understanding of the reactivity trends over the transition metals for this reaction requires two independent descriptors.[34] In Fig. 4, the 2-dimensional Sabatier volcano for the CO oxidation reaction over close-packed surfaces and high-temperature conditions is shown. Perhaps not surprisingly Pd and Pt turn out to be the best catalysts under these conditions.

We thus conclude that the BEP relations for surface reactions directly entail volcano relations for the catalytic rate as a function of surface reactivity, and that there is ample reason for describing the surface reactivity in terms of the dissociative chemisorption energy of the key reactants.[33]

Classification of structure sensitivity

The Sabatier analysis can be used to classify different types of structure sensitivity in catalytic reactions. Using the Sabatier analysis is equivalent to only considering reactions with a single well-defined rate limiting step. Systems with several such steps close to the top of the volcano where the real rate may deviate a little from the Sabatier rate may show interesting effects when several different sites can contribute and has been discussed in detail by Zhdanov and Kasemo.[35]

For simplicity, we will consider the case where a single adsorption energy can be used as a descriptor and where there are only two elementary steps to consider. The discussion below is easily generalized to the case with more elementary steps.

Fig. 5 proposes a classification of structure dependence of complete catalytic reactions. In the figure, we show BEP lines for the geometry probability-weighted activation energies, eqn (4), and the corresponding volcanoes. For two elementary steps, there are four possibilities depending on whether either elementary reaction shows strong structural effects or not according to the definition above. For simplicity, we only consider two different local geometries, defining the extremes in the structure dependence of the elementary reactions. The

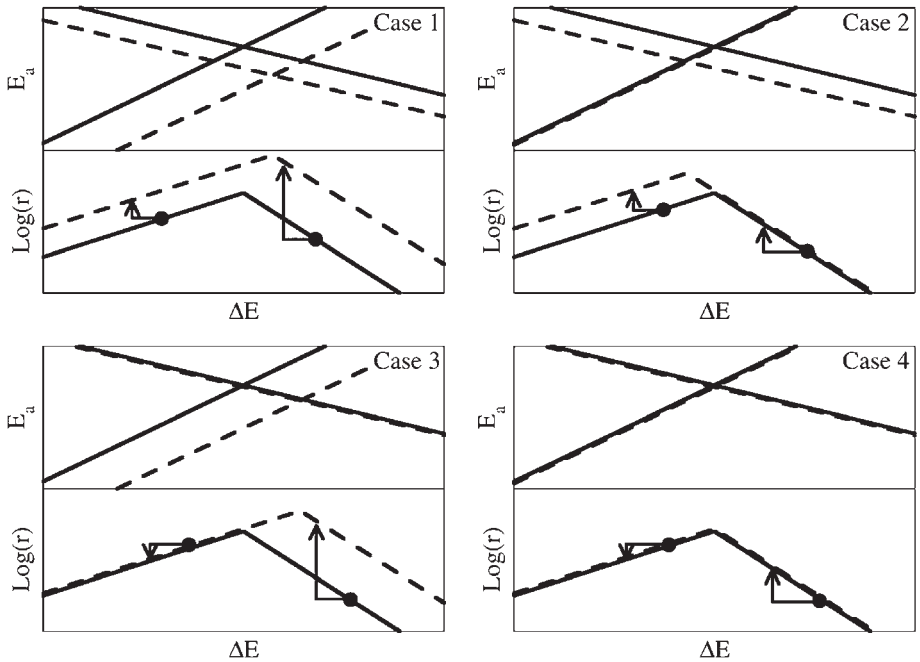

Fig. 5 A classification scheme of structure dependence for catalytic reactions. In each case the BEP lines for activation and removal are shown for two different sites. Below the BEP lines the resulting volcano types are shown. Case 1: both activation and removal exhibit structural dependence ($\delta\beta \gg \delta\Delta E$). Case 2: activation is independent of structure but removal shows structural dependence. Case 3: activation is structure dependent but removal is not. Case 4: neither activation nor removal shows structural dependence.

structure with the lowest BEP line (shown dashed in the figure) could be thought of as belonging to a step-like defect while the other could represent a close-packed surface. This reflects the line-ordering of the strongly bound diatomic molecules (*e.g.* NO, O_2, CO, and N_2); it will, however, in general depend on the reaction as to which surface structure has the lower-lying line.

In Fig. 5, the arrows indicate what happens to the rate over a given metal when going from a close-packed surface site to a step site where the adsorption energy is more exothermic. Fig. 5 suggests a set of rules for determining the nature of the active site. For metals on the right leg of the volcano (noble metals), the steps are always the most active. For the more reactive metals on the left leg, it depends on the degree of structure sensitivity of the elementary step whether the reaction will appear structure sensitive or not. For Case 3 and Case 4, the site that binds the intermediates most strongly has the lowest rate. This is what one would expect since on the left leg of the volcano, the rate-limiting step is the removal of the adsorbed intermediates. Here, the most reactive sites (in the sense of strongest bonding of surface intermediates) are self-poisoned by the reaction and do not contribute significantly to the catalytic rate. Case 1 and Case 2 are exceptions to this rule. Here the strongest bonding sites dominate because the reaction barrier is affected more than the reaction energy.

In the following section, we will discuss a number of explicit examples illustrating the classification above.

Examples

Fig. 6 shows the measured rate of methane dissociation on a Ni(111) surface with approximately 4% step sites when the surface is clean and when the steps have been blocked by adsorbed sulfur. Fig. 7a shows the same experiment but for CO dissociation. According to the discussion above, methane dissociation should show weak structural effects while CO dissociation should show strong structural effects. That is exactly what the data show. The rate of methane dissociation only differs by a factor of 140, which corresponds to a difference in activation barrier of approximately 0.2 eV, in excellent agreement with the calculations (see Fig. 1a). For CO dissociation, the surface where the steps are blocked shows no observable dissociation. Scanning tunneling microscopy

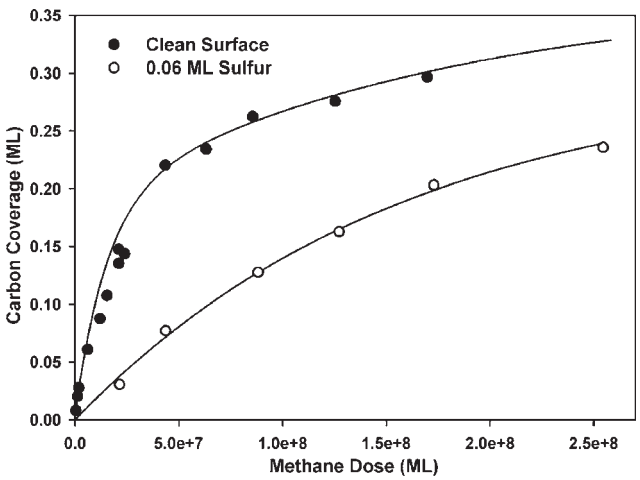

Fig. 6 Measured carbon deposits as a function of CH_4 dose at 500 K on a Ni(14 13 13) surface for two different cases; one case where the surface is "clean" (filled dots) and another where the step sites have been blocked by dosing 0.06 ML sulfur.[46]

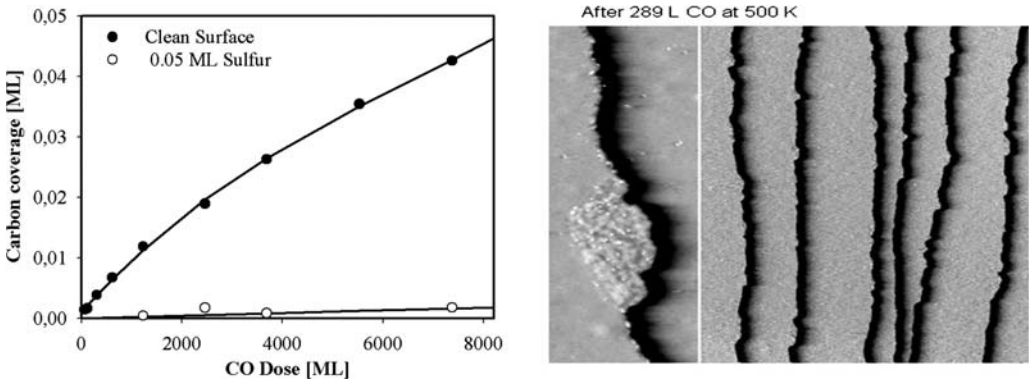

Fig. 7 The experimentally determined carbon coverage on a Ni(14 13 13) single crystal as a function of the CO exposure at 500 K. Results are shown for both the clean surface and for a surface that has been pre-exposed to 0.05 ML of sulfur which is known to preferentially block the steps. The surface is incapable of dissociating the CO when the steps are blocked. Adapted from ref. 47.

studies on a stepped Ni(111) surface after reaction with CO also show that the carbon deposits are exclusively formed along the steps, see Fig. 7b.

We note that a very strong structure dependence can appear in surface science experiments as an absence of structure sensitivity. If a defect like a step is the only active site and the nature of these defects are the same on different single crystal surfaces, then the rate will only depend on the number of these defects. Since the ratio of such defect sites is on the order of 1% due to the accuracy with which the crystal can be aligned and the entire polishing and cleaning procedure (and perhaps the area of the backside and edges of the crystal), the number of such sites may not vary much from one facet to the next. The rate of N_2 dissociation on Ru is an example of this behavior.[15] Fig. 8 shows the sticking of N_2 on a clean Ru(0001) surface with approximately 1% step sites. Blocking the steps by depositing small amounts of Au (1–2% of a monolayer) makes the sticking drop by roughly nine orders of magnitude, which clearly demonstrates the effects of the step sites. The open circle in Fig. 8 is the measured sticking of N_2 on Ru(0001),[36] which is identical to the sticking of N_2 found on the more open *Ru*(10$\bar{1}$0) and *Ru*(11$\bar{2}$1) surfaces.[37] Another example is N_2 dissociation over Fe. Given the data in Fig. 1b, the most straightforward explanation of the fact that Fe(110) is only 1–2 orders of magnitude slower at N_2 dissociation and ammonia synthesis than Fe(111)[38] is that there are a few percent of defect sites on the Fe(110) surface, which would otherwise be completely inactive. One of the important differences between ultra-high vacuum surface science experiments and "real" heterogeneous catalysis is that the catalytic reactions occur at significant gas pressures. This difference in conditions between surface science and catalysis is often referred to as the "pressure gap". An important aspect of the pressure gap is that the morphology of the catalytic particles might change significantly due to adsorbates from the reactive gas.[2] This change in morphology is often accompanied with a change in the relative abundance of different active sites. The relative abundance under reaction conditions is naturally the most relevant, but unfortunately also the most difficult to determine.

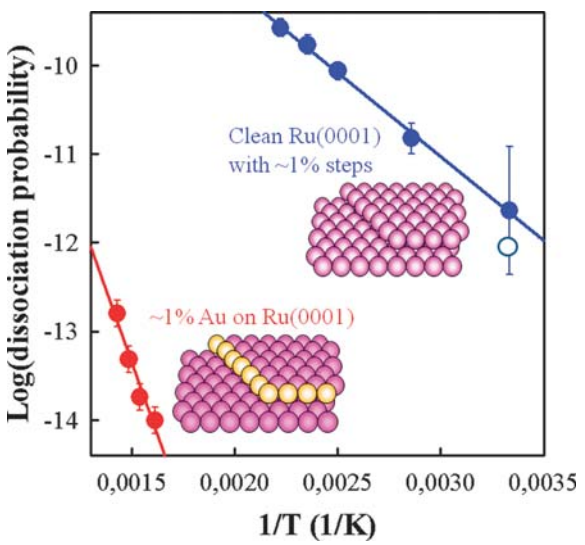

Fig. 8 Arrhenius plot of measured thermal sticking coefficients of N_2 on a clean Ru(0001) surface and the same surface covered with 0.01–0.02 ML of gold. The open circle is the result from a similar measurement at room temperature by Dietrich *et al.*[36]

Degree of structure sensitivity

The structure dependence of complete catalytic reactions over supported nanoparticle catalysts is often measured in terms of the dependence of the rate per exposed surface area, r, on the particle diameter, d:

$$\alpha = -\frac{\mathrm{d}\ln r}{\mathrm{d}\ln d} \tag{7}$$

If all surface sites contribute the same to the rate then $\alpha = 0$, meaning that the reaction step is structure insensitive. A value larger than zero indicates that the active site is of a lower dimensionality than the surface, that is, steps, edges, corners, or kinks, and α thus defines the "degree of structure sensitivity".

Using eqn (2) and (3), we can write that in terms of the contributions for different surface geometries as

$$\alpha = -\frac{d}{r}\frac{\mathrm{d}r}{\mathrm{d}d} = -\frac{d}{r}\nu\sum_i \frac{\mathrm{d}A_i}{\mathrm{d}d}\mathrm{e}^{-E_{\mathrm{a}i}/kT} = -\sum_i \frac{r_i}{r}\frac{\mathrm{d}\ln A_i}{\mathrm{d}\ln d} = \sum_i \frac{r_i}{r}\alpha_i \tag{8}$$

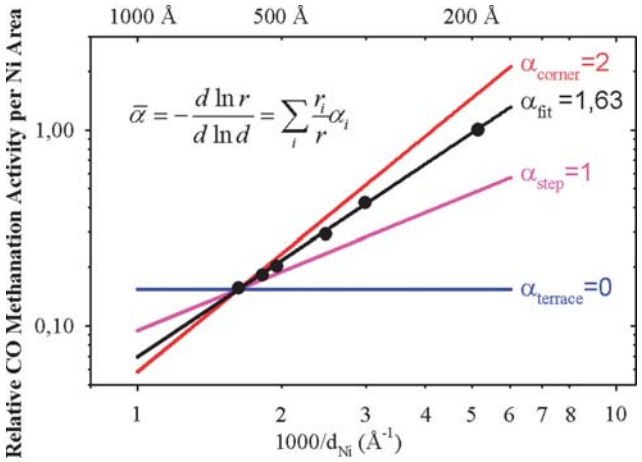

Fig. 9 Double-logarithmic plot of the relative CO methanation activity per Ni area of 1% CO in H_2 at 523 K and 1 bar plotted as a function of inverse particle size for a series of Ni catalysts with varying average particle size. The experimental points are best described by a line with a fitted slope (structure sensitivity) of 1.63. Adapted from ref. 47.

where α_i is a measure of the dimensionality of the sites of type i ($\alpha_i = 2 - N_{dimensions}$). Steps and edges (which are 1-dimensional) of a particle have $\alpha_i = 1$, whereas corners and kinks (which are point defects and therefore 0-dimensional) have $\alpha_i = 2$.

Fig. 9 shows experimental data for methanation. Here, CO dissociation is a necessary step in the reaction and as discussed above it is strongly structure dependent. The data in Fig. 9 indicate that both edges and corners of the metallic nanoparticles contribute to the rate, since the observed α is between one and two.

A number of other reactions belong to the same class of strongly structure dependent reactions. Ammonia synthesis is a good example. As would be expected from Fig. 1b, the ammonia synthesis shows a strong structure sensitivity.[39,40] Other well-established examples include the steam reforming process[41] and the dry reforming of propane to synthesis gas over Ni.[42] For steam reforming, an α value of 1 was observed for a number of metals indicating that even the weak structural effect of C–H bond splitting is sufficient to make low-coordinated metal atoms the active site.[41] For the dry reforming of propane the same may be true, but it may also be that for this reaction the C–C bond breaking is the rate limiting step and here we expect a strong structural effect. Recently, it was demonstrated by direct *in situ* characterization of the active sites that H_2 evolution over MoS_2 shows a strong structure sensitivity.[43]

There are cases illustrating how metals on two different sides of the volcano behave differently.[44,45] The electrochemical oxygen reduction reaction is such an example belonging to the class of reactions we refer to as "Case 3". Here, the removal of OH from the surface defines the left leg of the volcano, and the barrier for water formation is believed to be given essentially by the reaction energy. Hence, there is no structural shift in BEP lines for this reaction. As expected, Au on the right side of the volcano shows a clear increase in rate per surface area when going to smaller particles, whereas Pt on the left side has been measured to have a decrease in rate per surface area when the particle size decreases.

Summary and conclusions

Based on the Brønsted–Evans–Polanyi (BEP) relations obtained from electronic structure calculations of adsorption on metal surfaces, we have provided a molecular level discussion of the nature of the active sites in metal catalysis. It has been discussed how different classes of reactions result from the nature of their active sites and how these classes exhibit different dependence of their catalytic activity as a function of particle size. It was elaborated how the BEP relations determine the trends in catalytic activity from one metal to the next through the so-called volcano relationships. The dependence of the BEP lines on the local structure of the reaction site determines the structural (or geometrical) effect of the individual elementary reactions and it also determines whether a complete catalytic reaction is structure sensitive for a given catalyst. The BEP lines thus provide a tool to systematically decompose structure sensitivity into independent geometrical and electronic effects. The geometrical effect is the one described by the different vertical positions of the BEP lines corresponding to different sites, and the electronic effect is defined by the difference in adsorbate–surface interaction between different sites.

Acknowledgements

CINF and CSG are Danish National Research Foundation Centers and CAMD is a Center funded by the Lundbeck Foundation. The authors wish to acknowledge additional economic support from the Danish Research Agency through grant 26-04-0047 and from the Danish Center for Scientific Computing through grant HDW-0107-07.

References

1 T. W. Hansen, J. B. Wagner, P. L. Hansen, S. Dahl, H. Topsøe and C. J. H. Jacobsen, *Science*, 2001, **294**, 1508.
2 P. L. Hansen, J. B. Wagner, S. Helveg, J. R. Rostrup-Nielsen, B. S. Clausen and H. Topsøe, *Science*, 2002, **295**, 2053.
3 S. Hofmann, R. Sharma, C. Ducati, G. Du, C. Mattevi, C. Cepek, M. Cantoro, S. Pisana, A. Parvez, F. Cervantes-Sodi, A. C. Ferrari, R. Dunin-Borkowski, S. Lizzit, L. Petaccia, A. Goldoni and J. Robertson, *Nano Lett.*, 2007, **7**, 602.
4 L. C. Gontard, L.-Y. Chang, C. J. D. Hetherington, A. I. Kirkland, D. Ozkaya and R. E. Dunin-Borkowski, *Angew. Chem., Int. Ed.*, 2007, **46**, 3683.
5 H. S. Taylor, *Proc. R. Soc. London, Ser. A*, 1925, **108**, 105.
6 M. Boudart, *Adv. Catal.*, 1969, **20**, 153.
7 M. Boudart and G. Djéga-Mariadassou, *Kinetics of Heterogeneous Catalytic Reactions*, Princeton University Press, Princeton, New Jersey, 1984.
8 A. T. Gwathmey and R. E. Cunningham, *Adv. Catal.*, 1958, **10**, 57.
9 G. A. Somorjai, *Surface Chemistry and Catalysis*, Wiley, New York, 1994.
10 G. A. Somorjai, R. W. Joyner and B. Lang, *Proc. R. Soc. London, Ser. A*, 1972, **331**, 335.
11 D. W. Blakeley and G. A. Somorjai, *J. Catal.*, 1976, **42**, 181.
12 J. T. Yates Jr., *J. Vac. Sci. Technol., A*, 1995, **13**, 1359.
13 T. Zubkov, G. A. Morgan Jr., J. T. Yates Jr., O. Kühlert, M. Lisowski, R. Schillinger, D. Fick and H. J. Jänsch, *Surf. Sci.*, 2002, **526**, 57.

14 T. Zambelli, J. Wintterlin, J. Trost and G. Ertl, *Science*, 1996, **273**, 1688.
15 S. Dahl, A. Logadottir, R. C. Egeberg, J. H. Larsen, I. Chorkendorff, E. Törnqvist and J. K. Nørskov, *Phys. Rev. Lett.*, 1999, **83**, 1814.
16 H. S. Bengaard, J. K. Nørskov, J. Sehested, B. S. Clausen, L. P. Nielsen, A. M. Molenbroek and J. R. Rostrup-Nielsen, *J. Catal.*, 2002, **209**, 365.
17 R. T. Vang, K. Honkala, S. Dahl, E. K. Vestergaard, J. Schnadt, E. Lægsgaard, B. S. Clausen, J. K. Nørskov and F. Besenbacher, *Nat. Mater.*, 2005, **4**, 160.
18 M. Haruta, *Catal. Today*, 1997, **36**, 153.
19 M. Valden, X. Lai and D. W. Goodman, *Science*, 1998, **281**, 1647.
20 N. Lopez, T. V. W. Janssens, B. S. Clausen, Y. Xu, M. Mavrikakis, T. Bligaard and J. K. Nørskov, *J. Catal.*, 2004, **223**, 232.
21 A. S. K. Hashmi and G. J. Hutchings, *Angew. Chem., Int. Ed.*, 2006, **45**, 7896.
22 C. H. Christensen and J. K. Nørskov, *J. Chem. Phys.*, 2008, **128**, 182503.
23 W. Kohn, *Phys. Rev. Lett.*, 1996, **76**, 3168.
24 E. Prodan and W. Kohn, *Proc. Natl. Acad. Sci. U. S. A.*, 2005, **102**, 1135.
25 B. Hammer and J. K. Nørskov, *Nature*, 1995, **376**, 238.
26 B. Hammer and J. K. Nørskov, *Surf. Sci.*, 1995, **343**, 211.
27 B. Hammer and J. K. Nørskov, *Adv. Catal.*, 2000, **45**, 71.
28 T. Bligaard and J. K. Nørskov, in *Chemical Bonding at Surfaces and Interfaces*, ed. A. Nilsson, L. G. M. Pettersson and J. K. Nørskov, Elsevier, New York, 2008.
29 J. K. Nørskov, T. Bligaard, A. Logadottir, S. Bahn, L. B. Hansen, M. Bollinger, H. S. Bengaard, B. Hammer, Z. Sljivancanin, M. Mavrikakis, Y. Xu, S. Dahl and C. J. H. Jacobsen, *J. Catal.*, 2002, **209**, 275.
30 T. R. Munter, T. Bligaard, C. H. Christensen and J. K. Nørskov, *Phys. Chem. Chem. Phys.*, 2008, DOI: 10.1039/b720021h.
31 T. Bligaard, K. Honkala, A. Logadottir, J. K. Nørskov, S. Dahl and C. J. H. Jacobsen, *J. Phys. Chem. B*, 2003, **107**, 9325.
32 P. Sabatier, *Ber. Dtsch. Chem. Ges.*, 1911, **44**, 1984.
33 T. Bligaard, J. K. Nørskov, S. Dahl, J. Matthiesen, C. H. Christensen and J. Sehested, *J. Catal.*, 2004, **224**, 206.
34 H. Falsig, B. Hvolbæk, I. S. Kristensen, T. Jiang, T. Bligaard, C. H. Christensen and J. K. Nørskov, *Angew. Chem., Int. Ed.*, 2008, **47**, 4835.
35 V. P. Zhdanov and B. Kasemo, *J. Catal.*, 1997, **170**, 377.
36 H. Dietrich, P. Geng, K. Jacobi and G. Ertl, *J. Chem. Phys.*, 1996, **104**, 375.
37 K. Jacobi, H. Dietrich and G. Ertl, *Appl. Surf. Sci.*, 1997, **121–122**, 558.
38 G. Ertl, in *Catalytic Ammonia Synthesis: Fundamentals and Practice*, ed. J. R. Jennings, Plenum Press, New York, 1991.
39 S. R. Tennison, in *Catalytic Ammonia Synthesis: Fundamentals and Practice*, ed. J. R. Jennings, Plenum Press, New York, 1991.
40 C. J. H. Jacobsen, S. Dahl, P. L. Hansen, E. Törnqvist, H. Topsøe, D. V. Prip, P. B. Møenshaug and I. Chorkendorff, *J. Mol. Catal. A: Chem.*, 2000, **163**, 19.
41 J. M. Wei and E. Iglesia, *J. Phys. Chem. B*, 2004, **108**, 4094.
42 L. B. Råberg, M. B. Jensen, U. Olsbye, C. Daniel, S. Haag, C. Mirodatos and A. Olafsen Sjåstad, *J. Catal.*, 2007, **249**, 250.
43 T. F. Jaramillo, K. P. Jørgensen, J. Bonde, J. H. Nielsen, S. Horch and I. Chorkendorff, *Science*, 2007, **317**, 100.
44 K. J. J. Mayrhofer, B. B. Blizanac, M. Arenz, V. R. Stamenkovic, P. Ross and N. Markovic, *J. Phys. Chem. B*, 2005, **109**, 14433.
45 S. Guerin, B. E. Hayden, D. Pletcher, M. E. Rendall and J. P. Suchsland, *J. Comb. Chem.*, 2006, **8**, 679.
46 F. Abild-Pedersen, O. Lytken, J. Engbæk, G. Nielsen, I. Chorkendorff and J. K. Nørskov, *Surf. Sci.*, 2005, **590**, 127.
47 M. P. Andersson, F. Abild-Pedersen, I. N. Remediakis, T. Bligaard, G. Jones, J. Engbæk, O. Lytken, S. Horch, J. H. Nielsen, J. Sehested, J. R. Rostrup-Nielsen, J. K. Nørskov and I. Chorkendorff, *J. Catal.*, 2008, **255**, 6.